Toxicology Reports 8 (2021) 489–498

Contents lists available at ScienceDirect

Toxicology Reports

journal homepage: www.elsevier.com/locate/toxrep

VEGFR-2 kinase domain inhibition as a scaffold for anti-angiogenesis: Validation of the anti-angiogenic effects of carotenoids from *Spondias mombin* in DMBA model of breast carcinoma in Wistar rats

Damilohun Samuel Metibemu [a,b,*], Oluseyi Adeboye Akinloye [b], Adio Jamiu Akamo [b], Jude Ogechukwu Okoye [d], David Ajiboye Ojo [c], Eric Morifi [e], Idowu Olaposi Omotuyi [a]

[a] Department of Biochemistry, Adekunle Ajasin University, Akungba-Akoko, Ondo State, Nigeria
[b] Department of Biochemistry, Federal University of Agriculture, Abeokuta, Nigeria
[c] Department of Microbiology, Federal University of Agriculture, Abeokuta, Nigeria
[d] Department of Medical Laboratory Science, Faculty of Health Sciences and Technology, College of Medicine, Nnamdi Azikiwe University, Nnewi Campus, Nigeria
[e] Department of Chemistry, School of Chemistry, University of the Witwatersrand, Johannesburg, South Africa

ARTICLE INFO

Handling Editor: Dr. Aristidis Tsatsakis

Keywords:
VEGFR-2
Liquid Chromatography-Electrospray Ionization-Mass Spectrometry (LC-ESI-MS)
Angiogenesis
DFG-out conformation
7, 12-Dimethylbenz[a]anthracene (DMBA)
Spondias mombin

ABSTRACT

Vascular endothelial growth factor (VEGF) and its receptor-2 (VEGFR-2) mediated tumorigenesis, metastasis, and angiogenesis are the cause of the increased levels of mortality associated with breast cancer and other forms of cancer. Inhibition of VEGF and VEGFR-2 provides a great therapeutic option in the management of cancer. This study employed VEGFR-2 kinase domain inhibition as an anti-angiogenic scaffold and further validate the anti-angiogenic effects of the lead phytochemicals, carotenoids from *Spondias mombin* in 7, 12-Dimethylbenz[a] anthracene (DMBA) model of breast carcinoma in Wistar rats. Phytochemicals characterized from 6 reported anti-cancer plants were screened against the VEGFR-2 kinase domain. The lead phytochemicals, carotenoids from *Spondias mombin* were isolated and subjected to Liquid Chromatography-Electrospray Ionization-Mass Spectrometry (LC-ESI-MS) for characterization. The anti-angiogenic potentials of the carotenoid isolates were validated in the DMBA model of breast carcinoma in female Wistar rats through assessment of the expression of anti-angiogenic related mRNAs, histopathological analysis, and molecular docking. Treatment with carotenoid isolates (100 mg/kg and 200 mg/kg) significantly ($p < 0.05$) downregulated the expression of VEGF, VEGFR, Epidermal Growth Factor Receptor *(EGFR),* Hypoxia-Inducible Factor-1(*HIF-1*), and Matrix Metalloproteinase-2 *(MMP-2*) mRNAs in the mammary tumours, while the expression of Chromodomain Helicase DNA-Binding Protein-1 (CHD-1) mRNA was significantly ($p < 0.05$) upregulated. DMBA induced comedo and invasive ductal subtypes of breast carcinoma. The binding of astaxanthin, 7,7',8,8'-tetrahydro-β,β-carotene, and beta-carotene-15,15′-epoxide to the ATP binding site led to the DFG-out conformation with binding energies of -8.2 kcal/mol, -10.3 kcal/mol, and -10.5 kcal/mol respectively. Carotenoid isolates demonstrated anti-angiogenic and anti-proliferating potentials via VEGFR-2 kinase domain inhibition.

1. Introduction

Breast cancer is the most prevalent cancer in women [1]. Breast cancer will be diagnosed in 12 % of all women over their lifespan [1]. Mutation in genes that are responsible for cell cycle progression and subsequent loss of regulatory cell functions are responsible for the majority of breast cancer. Angiogenesis, the process of sprouting, cell division, migration, and assembly of endothelial cells (ECs) from pre-existing vessels [2] is a key player in the growth of cancer cells and one of the main causes of death from breast cancer [3]. The role of angiogenesis in tumor growth and metastasis has been established [3]. It plays a central role in embryogenesis and postnatal events including wound healing, the female reproductive cycle, and chronic inflammation [4]. In a normal cell, angiogenesis can be turned off and on but in neoplastic cells, it is perpetually turned on. The vascular endothelial growth factor (VEGF) and its receptor (VEGFR) are responsible for vasculogenesis and angiogenesis [5]. The seven members of VEGF include the VEGF-E, VEGF-A, and its receptors VEGFR-1 and VEGFR-2

* Corresponding author at: Department of Biochemistry, Adekunle Ajasin University, Akungba-Akoko, Ondo State, Nigeria.
E-mail address: damilohun.metibemu@aaua.edu.ng (D.S. Metibemu).

https://doi.org/10.1016/j.toxrep.2021.02.011
Received 9 April 2020; Received in revised form 18 February 2021; Accepted 20 February 2021
Available online 25 February 2021

control both physiological and pathological conditions. VEGF-C and D and their receptor VEGFR-3 control lymphangiogenesis and embryonic development [5]. The signal transduction cascades are set in motion when VEGF-A binds to VEGFR-1 (Flt-1) and VEGFR-2 (KDR/ Flk-1). VEGFR-2 is mainly responsible for the pro-angiogenic functions of the VEGFRs [5]. The VEGFR-2 carries signal transduction via the phosphatidylinositol-3-kinase/protein kinase B(PI3K/Akt) pathway [6]. VEGF and VEGFR-2 mediated tumorigenesis, metastasis, and angiogenesis are culpable in the high level of mortality associated with breast cancer and other forms of cancer [2]. The angiogenic process can be forestalled by either preventing the VEGF from binding to its receptors [7] and or inhibiting the phosphorylation of the tyrosine kinase domain by small molecules [7]. Small molecule inhibitors of the tyrosine kinase domain disrupt the activation of the receptor tyrosine kinases by preventing ATP binding. Natural compounds have been reported to inhibit the tyrosine kinase domain and also demonstrate antiangiogenic properties [5,8]. With the prevailing patients resistant to chemotherapeutic drugs, it imperative to come up with novel drugs particularly of plant origin considering the critical roles natural products (plants) play in the discovery and development of new pharmaceuticals [9].

The use of plants for medical purposes is from time immemorial [9]. Modern drug discovery has incorporated the use of medicinal plants due to their perceived non-toxicity to normal cells and tolerability to the drug development pipeline [9. Phytochemicals have been reported to explore different mechanisms in their antitumor properties [10,11]. They selectively destroy proliferating cancerous cells, target anomaly expressed molecular factors, expunge oxidative stress, mediate cell growth factors, obstruct angiogenesis of cancerous tissue, and induce apoptotic cell death [10].

It is important to adopt computational procedures in hit-to-lead optimization, to reduce cost, time, and cover a large number of drug-like candidates from the pool of plant-derived phytochemicals [12]. Virtual High Throughput Screening (vHTS) is a globally recognized alternative method to High Throughput Screening (HTS), a computational procedure of searching small molecule libraries for molecules that will bind drug targets [13].

In this study, the anti-angiogenic potentials of six reported anti-cancer plants, *Anacardium occidentale*, *Ocimum gratissimum*, *Momordica charantia, Spondias mombin*, *Piper guineese,* and *Gongronema latifolium* were queried by vHTS against VEGFR-2 kinase domain as a scaffold for anti-angiogenesis. Carotenoids from *Spondias mombin* were the hit phytochemicals, and thus, they were isolated from the leaves of the plant, and their antiangiogenic effects were validated in 7, 12-Dimethylbenz[a]anthracene (DMBA) model of breast carcinoma in female Wistar rats.

2. Methodology

2.1. Data collection and preparation of target protein

Three hundred and twenty-three (323) phytochemicals that were characterized from six reported anti-cancer plants, *Anacardium occidentale, Ocimum gratissimum, Momordica charantia, Spondias mombin*, *Piper guineese, Gongronema latifolium* [14–19] were obtained from the literature [23–28]. Phytochemicals were downloaded in the Structure data format (SDF format) from the PubChem repository (https://pubchem.ncbi.nlm.nih.gov) and were converted to the protein data bank (PDB) and protein data bank charged (PDBQT) formats respectively. The crystal structure of the human VEGFR-2 kinase domain with a novel pyrrolopyrimidine inhibitor (crystallographic resolution of 1.55 Aº and PDB ID: 3VHE) [20] was downloaded from the protein data bank (http://www.rcsb.org).

Command lines;

```
% babel H.sdf H.pdb -h -r -m –gen3D
% for i in {1..50}; do ligprep -l H${i}.pdb -o H${i}.pdbqt
```

Where; H is the name of the file (that contains the phytochemicals).

1..50 indicate the number of phytochemicals in the file

2.2. Virtual high throughput screening and molecular docking

Virtual High Throughput Screening (vHTS) was used to screen phytochemicals from *Anacardium occidentale, Ocimum gratissimum, Momordica charantia, Spondias mombin Piper guineese, Gongronema latifolium* against the ATP-binding pocket of VEGFR-2 (3VHE). The grid coordinates (X= -24.97, Y=-1.14, Z=-10.52) of the co-crystallized compound were used.

2.3. Isolation of lead compounds and LC-ESI-MS analysis

The lead phytochemicals, carotenoids from *Spondias mombin* leaves were extracted, isolated, and characterized according to the methods earlier reported by Rodriguez, (2001) [21] and Metibemu et al., 2020 [22].

2.4. Experimental animals

The G*Power 3 software [23] was used to determine the sample size of 30 female Wistar rats. Wistar rats between 40–50 days old were used for the experiment. The animals were acclimatized for two weeks before the induction of DMBA. The study was carried out with strict adherence to standard protocols of handling experiment animals. The experimental protocols were assessed and endorsed by the Institutional Animal Ethics Committee (IAEC).

2.5. Experimental design

The Wistar rats were randomized into 6 groups of 5 Wistar rats per group. Group 1 (control), received normal chow and water only. Groups 2–5 were induced intra-peritoneally (IP) with a single dose of 35 mg/kg of DMBA. Groups 3−5 were treated (Per os (p.o): administration through the mouth) for 4 weeks (after confirmation of mammary tumour in all the Wister rats) with 100 mg/kg carotenoid isolates, 200 mg/kg carotenoid isolates, and 100 mg/kg carotenoid isolates +100 mg/kg celecoxib respectively. Group 6 (without tumour induction with DMBA) was also treated with 200 mg/kg carotenoid isolates. The detailed experimental design is shown in Fig. 1.

Celecoxib (an FDA approved COX-2 inhibitor) was introduced in group 5 to determine the combinatorial therapeutic effects of targeting both COX-2 and VEGFR-2 receptors in the DMBA model of breast carcinoma in Wistar rats. COX-2 expression is reported to be associated with angiogenesis and lymph node metastasis in human breast cancer [24].

The doses of carotenoid isolates and DMBA employed for the present study were informed by previous studies [22,25].

2.6. Tumor induction

The method of Baross et al. (2004) [26] for DMBA induction of mammary tumour was adopted. The animals were administered intraperitoneally with a single dose of 35 mg/kg bodyweight of DMBA dissolved in corn oil. Tumour formation was observed after 24 weeks in all the Wistar rats. The animals were sacrificed and anaesthetized by cervical dislocation.

2.7. Tumour volume

The method proposed by Geran et al. (1972) [27] was used to determine the tumour volume. The measurement was carried out with the aid of Vernier calipers.

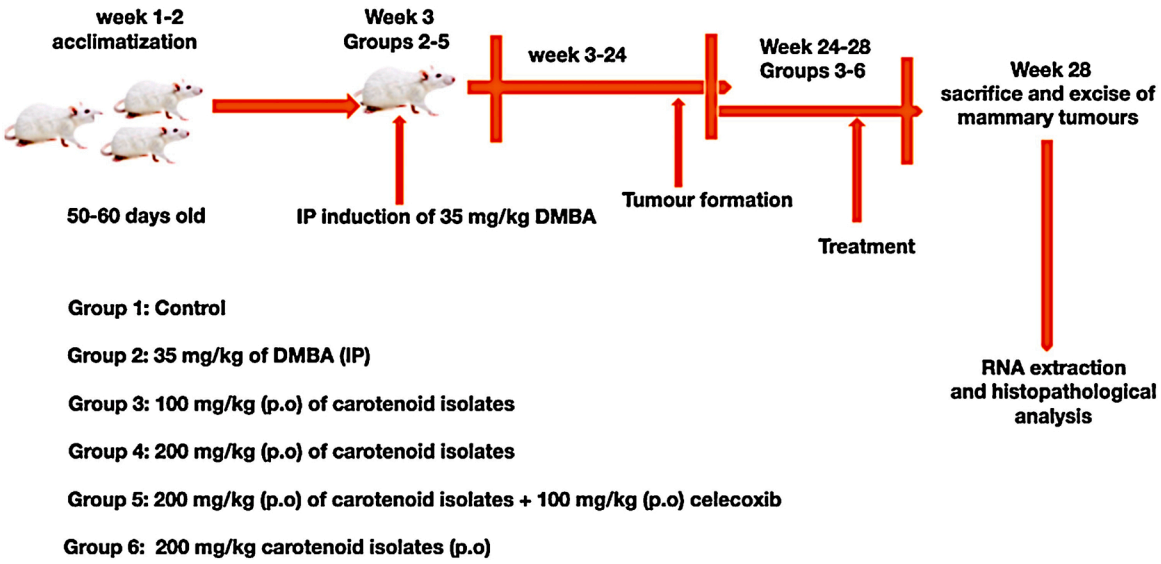

Fig. 1. Experimental design to validate the anti-angiogenic effects of carotenoids from *Spondias mombin*.

2.8. Reverse transcription-polymerase chain reactions

Trizol reagent (Gibco) was used to isolate the RNA from the mammary tumour. The RNA-free DNase (Roche, Switzerland) was used to dissolve the RNA for 15 min. at a temperature of 37 °C and purified with the RNeasy kit (Qiagen, Germany). The cDNA was synthesized by incubating 40 μg of the total RNA at 37 °C for 1 h with the reverse transcriptase (GE Healthcare, UK) and also with random hexanucleotides, following the manufacturer's instructions. The Primers of interest were designed by the Snap gene software. The Primers were ordered from Sigma-Aldrich, USA. Glyceraldehyde-3-phosphate *(GAPDH)* was used as the control gene. The amplification of the genes was done for 50 cycles, 2 h 20 min with the aid of a thermocycler. The PCR products were run on 1.0 % agarose gels. Visualization was carried with the aid of ethidium bromide (EtBr) staining [28]. The primers of interest are;

TARGET GENES	FORWARD 5′-3′	REVERSE 5′-3′
MMP-2	GCAGCCTAGCCAGTCGGATTT	CCACGTGACAAGCCATGGGGCCCC
GAPDH	AAGGGCTCATGACCACAGTC	GGATGCAGGGATGATGTTCT
CHD1	GTTCTTCGGGGAACAGAGCGA	GTCCTCGTGAGCAATGACCA
VEGF	TGTGGGCTATGAGCCAAGTG	CAACCGTGAGAGCAAGCAAC
EGFR	GATTAATCCCGGAGAGCCAGA	TGAGCCTGTTACTTGTGCCT
VEGFR	TGTGGGCTATGAGCCAAGTG	CAACCGTGAGAGCAAGCAAC
HIF-1	GTTTACTAAAGGACAAGTCACC	TTCTGTTTGTTGAAGGGAG

2.9. Haematoxylin and Eosin for general histoarchitecture of the tumours

The harvested mammary tumour samples were immersion-fixed in 10 % formo-saline. Water was run through the sample overnight to remove the fixative. After the samples were dehydrated, they were subsequently cleaned in methyl-benzoate. The samples were later immersed in paraffin wax. They were cut (3–5 μm thickness) and stained with hematoxylin and eosin. These were then photomicrographed for viewing of the resultant histoarchitecture.

2.10. Molecular docking of the phytoconstituents of carotenoid isolates

Liquid chromatography–mass spectrometry (LC–MS) characterized carotenoid isolates; astaxanthin, beta-carotene-15,15′-epoxide, and 7,7′,8,8′-Tetrahydro-beta, beta-carotene were docked into the ATP pocket of VEGFR-2 (3VHE). Grid coordinates of the co-crystallized compounds X=-24.97, Y=-1.14, Z=-10, was adopted.

2.11. Statistical analysis

One-way analysis of variance (ANOVA) and Turkey's multiple range tests in IBM-SPSS version 21.0 and GraphPad Prism version 7.0 were used. Data were denoted as the means ± standard error of the mean (SEM). Significance was set at $p < 0.05$.

3. Results

3.1. Virtual high throughput screening reveals carotenoids as leads

Tables 1–3 shows the docking scores of some of the 323 phytochemicals characterized from *Anacardium occidentale, Ocimum gratissimum, Momordica charantia*, *Spondias mombin, Piper guineese, and Gongronema latifolium* screened against the ATP catalytic domain of VEGFR-2 with PDB ID of 3VHE. The lead compounds from the virtual screening herein show alpha-carotene, beta-carotene, and beta-cryptoxanthin with a docking score of 11.3 kcal/mol, 11.1 kcal/mol, and 10.7 kcal/mol respectively from *Spondias mombin.* It is worthy of note that the lead compounds are carotenoids.

Table 1
Docking scores of Phytochemicals characterized from *Anacardium occidentale* and *Ocimum gratissimum* when screened against the catalytic domain of VEGFR-2.

Anacardium occidentale			*Ocimum gratissimum*	
S/N	Phytochemicals	Docking Scores	Phytochemicals	Docking scores
1	Actinidine	−6.2	1-Heptacosanol	−6.6
2	Adipostatatin A	−7.3	1-Octen-3-ol	−5
3	Anthranilic acid	−5.6	1-Phenyldecane	−6.9
4	Atisine	−9.4	Alloaromadendrene	−7.1
5	Atropine	−7.7	Alpha-Panasinsen	−7.4
6	Berberine	−7.6	Alpha-Pinene	−6.5
7	Bicuculine	−8.1	Alpha-Terpinene	−6.4
8	Brucine	−6.9	Alpha-Terpineol	−6.4
9	Cardanol	−7.4	Aromadendrene	−7.2
10	Carpaine	−6.5	Azulene	−6.8

Table 2
Docking scores of Phytochemicals characterized from *Momordica charantia* and *Spondias mombin* when screened against the catalytic domain of VEGFR-2.

Momordica charantia			*Spondias mombin*	
S/N	Phytochemicals	Docking scores	Phytochemicals	Docking scores
1	3-beta hyroxy 2 oxomanoyloxide	−7.5	Alpha-carotene	−11.3
2	4-beta, 5-alpha-epoxy-4,5-dihydrocaryophyllene-14-ol	−7.5	Alpha-cubebene	−7
3	6,7,8 trimethoxycoumarin	−6.3	Alpha-terpineol	−6.2
4	Allicin	−4.2	Amydalin	−6.7
5	Alpha-bulnesene	−6.6	Berberine	−7.7
6	Apha-elemene	−6.5	Beta-carotene	−11.1
7	Alpha-gualene	−6.8	Beta-caryopyllene	−7
8	Aplha-humulene	−7.2	Beta-cryptoxanthin	−10.7
9	Beta-bulnesene	−6.7	Caffeic acid	−6.5
10	Beta-gualene	−8	Caffeine	−5.8

Table 3
Docking scores of Phytochemicals characterized from *Piper guineese* and *Gongronema latifolium* when screened against the catalytic domain of VEGFR2.

Piper guineese			*Gongronema latifolium*	
S/N	Phytochemicals	Docking score	Phytochemicals	Docking score
1	Allo-Aromadendrene	−7.7	3, 4-Dihyroxyphenylacetic acid	−5.9
2	Aloe-emodin	−8	4-(-ethoxymethyl)-phenol	−5.6
3	Aloin	−8.5	4-hydroxybenzaldehyde	−5.2
4	Alpha-bergamotene	−8.3	Afrocylamin A	−0.5
5	Alpha-phellandrene	−6.3	Afrocylamin B	−3.2
6	Asimicin	−9.1	Alpha-phellandrene	−6.3
7	Azadirachtin	1.1	Alpha-terpinene	−6.4
8	Beta-caryophyllene	−7.3	Astraodoric acid D	−5.9
9	Beta-Pinene	−6.2	Benzaldehyde	−5
10	Borneol	−6.5	Beta-amyrin	−7.2

3.2. The leads inform the isolation of carotenoids from Spondias mombin leaves

As revealed from the vHTS of phytochemicals from the selected plants (Tables 1–3). The lead compounds, alpha-carotene, beta-carotene, and beta-cryptoxanthin with docking scores of 11.3 kcal/mol, 11.1 kcal/mol, and 10.7 kcal/mol respectively (Tables 1–3) are carotenoids from *Spondias mombin*. Hence the extraction and isolation of carotenoids from the leaves of *Spondias mombin*.

3.3. LC-ESI-MS revealed three carotenoids from Spondias mombin leaves

Beta-carotene-15,15′-epoxide, astaxanthin, and 7,7′,8,8′-tetrahydro-β-β-carotene were identified from the LC-ESI-MS analysis of carotenoids isolated from *Spondias mombin* leaves [Table 4] [22].

3.4. Tumour formation and tumour volume

The formation of tumour (Fig. 2) was observed after 24 weeks following a single intraperitoneal induction of 35 mg/kg bodyweight of DMBA. The Wistar rats were thereafter treated for 4 weeks. Fig. 3A and B show the excised mammary tumours and graph of tumor volumes respectively in the DMBA model of breast carcinoma in Wistar rats. In Fig. 3B, there is no significant difference between group 2 and group 3. There is a significant difference between group 2 and group 3. A significant difference also exists between group 2 and group 5.

3.5. mRNAs expression of angiogenic related genes in the mammary tumours of DMBA-model of breast carcinoma following treatment with carotenoid isolates

3.5.1. Relative expression of VEGF mRNA

VEGF is the principal mediator of angiogenesis in cancer, it is upregulated by oncogene expression, growth factors, and hypoxia. Angiogenesis is essential for neoplastic proliferation and growth [32].

In Fig. 4A, there was a significant downregulation in the expression of *VEGF* mRNA in group 3, group 4, group 5, and group 6 when compared with group 1, and group 2.

3.5.2. Relative expression of VEGFR mRNA

VEGFR and *VEGF* are co-expressed in primary breast carcinoma with further upregulation of *VEGFR* when neoplastic cells become angiogenetic phenotype [33].

In Fig. 4B, there was a significant downregulation in the expression of *VEGFR* mRNA in group 3, group 4, group 5, and group 6 when compared with group 2.

3.5.3. Relative expression of EGFR mRNA

EGFR is expressed in malignant and nonmalignant cells; however, it is upregulated in multiple forms of tumors. The expression of *EGFR* corresponds with poor response to treatment, disease progression, and poor survival [34].

In Fig. 4C, the expression of *EGFR* mRNA was significantly downregulated in group 3, group 4, group, and group 6 when compared to group 2. There was a significant downregulation in EGFR mRNA expression in group 3 when compared to group 1.

3.5.4. Relative expression of HIF-1 mRNA

HIF-1 displays principal roles in energy metabolism, apoptosis, angiogenesis, and control homeostatic reaction to hypoxia [35].

In Fig. 4D, the expression of *HIF-1* mRNA was significantly downregulated in group 3, group 4, group 5, and group 6 when compared with group 1.

3.5.5. Relative expression of CHD1 mRNA

E-cadherin (CDH1) is a cell adhesion molecule that organizes pivotal morphogenetic processes regulating neoplastic development. A decreased level of CDH1 is a characteristic of the epithelial–mesenchymal transition, leading to an increase in the metastatic power of malignant cells [36].

In Fig. 4E, the expression of *CDH1* mRNA was significantly upregulated in groups 4 and 5 when compared with groups 1 and 2. The expression of *CDH1* mRNA was upregulated in group 3 when compared with group 2, though not statistically significant at $p < 0.05$. However,

Table 4
Carotenoid fragments obtained with positive ionization mode from *Spondias mombin* leaves.

Peak no.	Identification	Elemental Composition	Molecular ion [M+H+]	MS/MS Fragmentation (positive ion mode) M/Z	References
a	Astaxanthin	$C_{40}H_{52}O_4$	600	311,283,166,88	[29]
b	Beta-Carotene-15,15'-epoxide	$C_{40}H_{56}O$	552	429,307,81	[29,30]
c	7,7',8,8'-Tetrahydro-beta, beta-carotene	$C_{40}H_{60}$	540	311, 165, 102	[31]

Fig. 2. Breast carcinoma in female Wistar rats induced with DMBA.

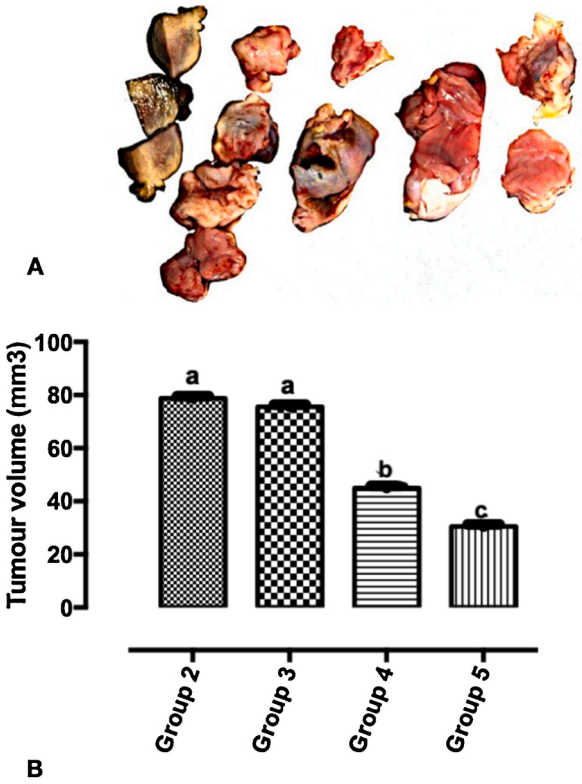

Fig. 3. A. The excised mammary tumours. B: Graph of tumor volumes in the DMBA-induced breast carcinoma model of Wistar rats in the different experimental groups. Values are expressed as Mean ± Standard Error of Mean (n = 5/group). Significance was set at $p < 0.05$. The non-identical alphabets on the bars indicate a significant difference.

the expression of *CDH1* was significantly upregulated in groups 3, 4, 5, and 6 when compared with the basal control (group 1).

3.5.6. Relative expression of MMP-2 mRNA

The *MMP-2* mRNA directs the translation of Matrix Metallopeptidase 2. They are activated through hydrolysis and cause the degradation of the basement membrane (BM) and attenuating the ability of BMs to hinder tumor cell migration. MMP-2 plays a key role in the degradation of the extracellular matrices and encouraging tumor invasion and metastasis [37].

In Fig. 4F, *MMP-2* mRNA was significantly expressed in group 2 when compared to group 1, the expression of *MMP-2* mRNA was significantly downregulated in groups 3, 4, 5, and 6 when compared to group 2. There was a significant upregulation in the expression of *MMP-2* mRNA in groups 3, 4, 5, and 6 when compared to group 1.

3.6. Histopathological analysis

The breast tumours were biopsied and stained with hematoxylin and eosin (H&E) to accentuate various tissue structures; nuclei and cytoplasm. Fig. 5 shows the histopathological sections of the breast tumours.

Group 1 (control) had normal mammary lobes with non-malignant acini. Group 2 had spindle-shaped cells and atypical features consistent with sarcomatoid lesions and Comedo carcinoma. Group 3 developed invasive ductal carcinoma while the breast tissues of group 4 had evidence of moderate to extensive necrosis and inflammatory cells. Group 5 had a nest of malignant glands demarcated by a delicate fibrous tissue while group 6 also had non-malignant mammary lobes.

3.7. Molecular docking of carotenoid isolates into the ATP-binding pocket of VEGFR-2

Inhibitors of the tyrosine kinase domain disrupt the activation of the receptor tyrosine kinase (RTKs) by inhibiting ATP binding [5]. Table 5 shows the docking results of the carotenoid isolates within the ATP binding site. Beta-carotene-15,15′-epoxide, 7,7′,8,8′-tetrahydro-β,β-carotene, and astaxanthin possess binding energies of -10.5 kcal/mol, -10.3 kcal/mol, and -8.2 kcal/mol respectively (Table 5). Fig. 6 shows the crystal structure of the VEGFR-2 kinase domain in complex with the standard drug, axitinib, and carotenoid isolates (Beta-carotene-15,15′-epoxide, 7,7′,8,8′-Tetrahydro-β,β-carotene, and Astaxanthin). Fig. 7 shows the validation of the docking protocols employed in the present study.

4. Discussion

4.1. Virtual high throughput screening of phytochemicals from selected plants

vHTS of 323 phytochemicals from the reported anti-cancer Plants; *Anacardium occidentale*, *Ocimum gratissimum*, *Momordica charantia*, *Spondias mombin*, *Piper guineese*, *Gongronema latifolium* revealed alpha-carotene, beta-carotene, and beta-cryptoxanthin with a docking score of 11.3 kcal/mol, 11.1 kcal/mol, and 10.7 kcal/mol (Table 3) respectively from *Spondias mombin* as the lead compounds. The lead compounds alpha-carotene, beta-carotene, and beta-cryptoxanthin are carotenoids. It suffices to say that carotenoids generally have been proven to possess anti-carcinogenic activities in several tissues [38,39]. The discovery of novel bioactive compounds with therapeutic benefits as obtained from the Virtual High Throughput Screening (vHTS) procedures adopted herein corroborated the significance of computer-aided drug design in the drug discovery pipeline [40].

4.2. Liquid chromatography-electrospray ionization-mass spectrometry and metabolomics analysis

The carotenoids isolated from the leaves of *Spondias mombin* were chromatographically separated into two fractions and afterward identified using Liquid Chromatography-Electrospray ionization-Mass Spectrometry. Compounds annotation was carried out based on the

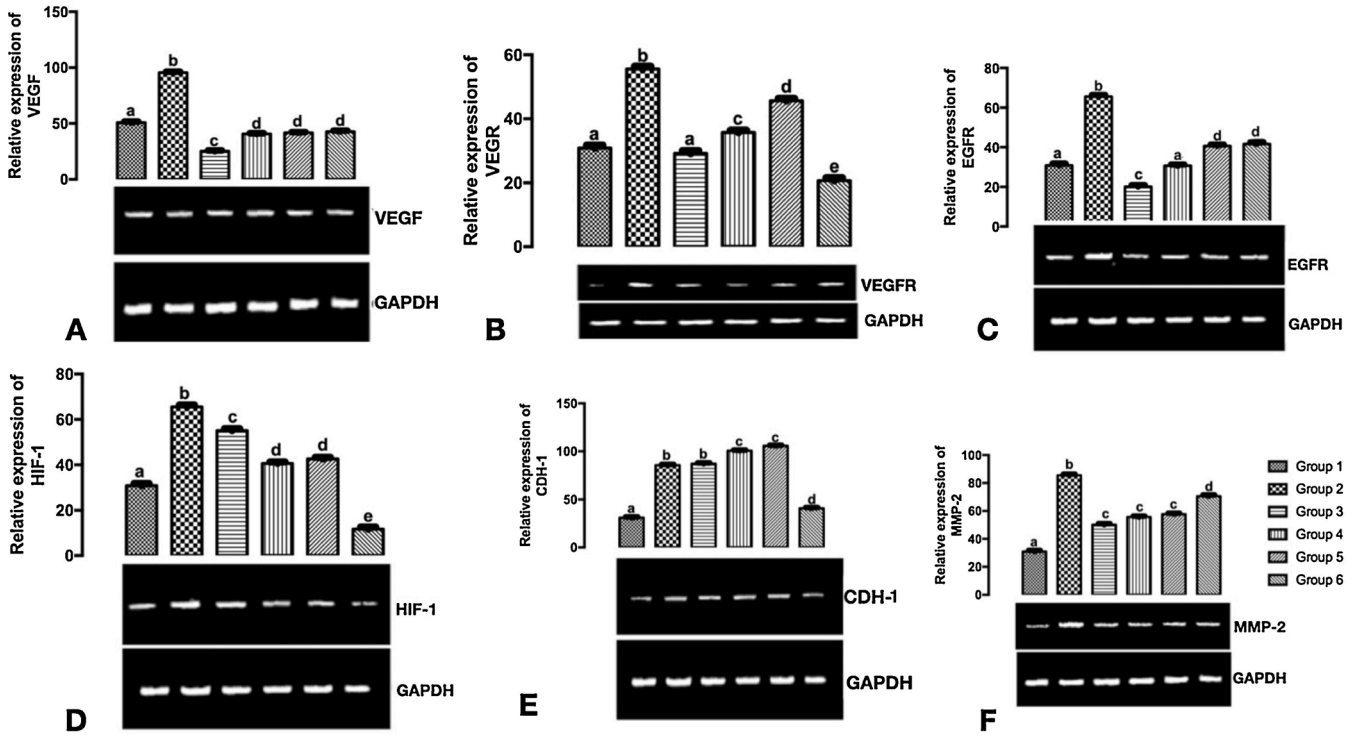

Fig. 4. mRNAs expression of angiogenic related genes in the mammary tumours of DMBA-model of breast carcinoma following treatment with carotenoid Isolates A: *VEGF* mRNA B: *VEGR* mRNA C. *EGFR* mRNA D: *HIF-1* mRNA. E: *CHD1* mRNA F: MMP-2 mRNA. Bars with different alphabets are significantly different at $p < 0.05$.

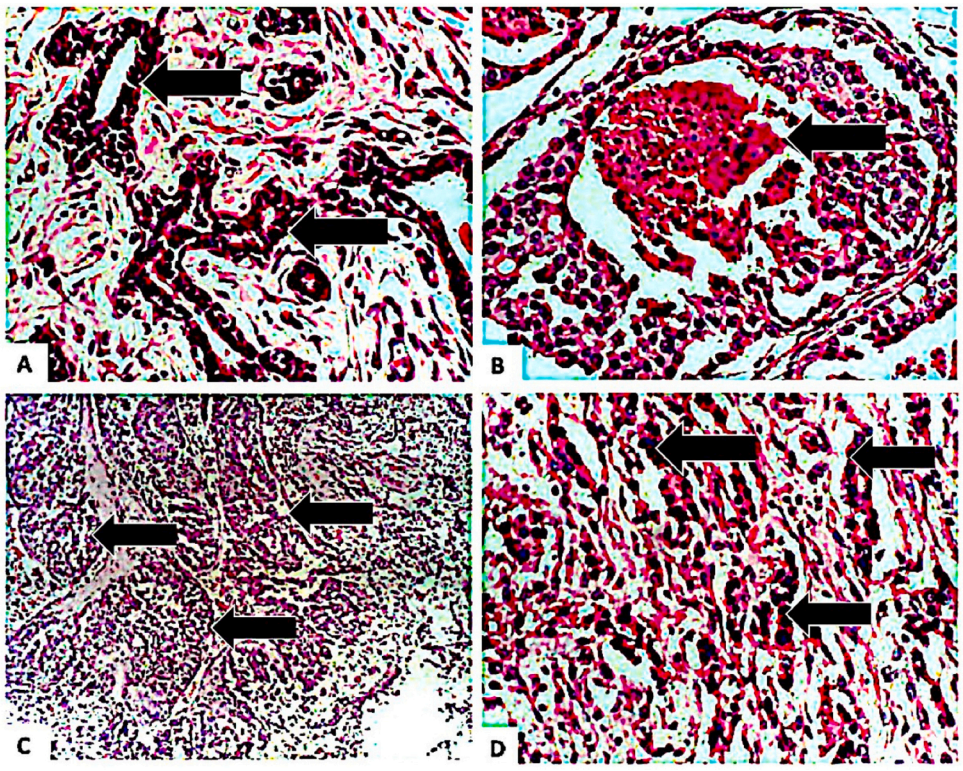

Fig. 5. Photomicrograph of a non-malignant mammary lobe in breast tissue marked by black arrows (A), photomicrograph of non-infiltrating and intraductal tumours with central necrosis (marked by black arrow) and consistent with Comedo carcinoma (B), photomicrograph shows nests of malignant glands consistent with invasive ductal carcinoma (marked by arrows; C), intra- and inter-acini pleomorphic and hyperchromatic cells with high nuclear-cytoplasmic ratio (D). Haematoxylin and Eosin (H&E) stained. Magnification: X20 (A, B, and D; from test groups) and X5 (C; from the control group).

recommendation of the Metabolomics Society by combining information obtained from mass spectra characteristics, literature, and or databases [41]. The chromatogram of the carotenoids and positive ion electrospray ionization Mass Spectrometry fragmentation patterns show the presence of three (3) carotenoids [22]. Carotenoids tend to form stable protonated molecules ($[M+H]^+$) with the positive mode of

Table 5
Docking score of the carotenoid isolates within the kinase domain of VEGFR-2.

Carotenoid Isolate/Standard drug	VEGFR-2
Astaxanthin	−8.2 kcal/mol
7,7′,8,8′-Tetrahydro-β,β-carotene	−10.3 kcal/mol
Beta-Carotene-15,15′-epoxide	−10.5 kcal/mol
Axitinib	−9.6 kcal/mol

ionization, hence the analysis of the sample in the positive mode. Peak I was not identified in part due to the lower *m/z* 121 which is believed to be a non-carotenoid compound. Peak 2 with *m/z* 600 $[M+4\ H]^+$ and fragmentation (311,283,166,88) corresponds to astaxanthin [29]. Peak 3 with *m/z* 552 $(M+H)^+$ and fragmentation (429,307,81) corresponds to beta-Carotene-15,15′-epoxide [30]. Lastly, peak 4 with *m/z* 540 $(M+H)^+$ and fragmentation (311, 165, 102) corresponds to 7,7′,8,8′-Tetrahydro-beta, beta-carotene [31].

4.3. Angiogenic-related mRNAs expression profiling

VEGF is an indispensable moderator of angiogenesis. Angiogenesis is important for neoplastic development and growth. The upregulation of VEGF mRNA commits the neoplastic cells to exponential growth. VEGF is central to tumour vasculature and survival 42]. The expression of VEGF mRNA was significantly downregulated in groups 3, 4, 5, and group 6 when compared with group 2. The significant downregulation of the VEGF mRNA expression by the carotenoid isolates (groups 3–6) depicts the anti-angiogenic properties of carotenoids, this is in agreement with the report of Kuhnen et al. (2009) [43] that carotenoids possess anti-angiogenic properties. The significant downregulation of *VEGFR* mRNA by the carotenoid isolates in groups 3–6, when compared with group 2 give credence to the inhibition of the Kinase Domain Receptor (KDR) of VEGFR as obtained from the Virtual Screening adopted in the present study.

Epidermal growth factor receptor (EGFR) is a pivotal factor in neoplastic malignancies, and its activity promotes tumor growth, invasion, and metastasis [44]. The *EGFR* mRNA is over-expressed in different forms of carcinoma including breast carcinoma [44]. The expression of the *EGFR* mRNA was significantly downregulated in all the treatment groups (3−5) and group 6 when compared with group 2. The degree of

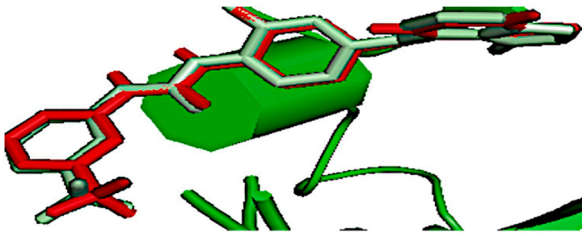

Fig. 7. The binding mode of the re-docked (red) and the co-crystallized, 1-{2-fluoro-4-[(5-methyl-5H-pyrrolo[3,2-d] pyrimidin-4-yl) oxy] phenyl}-3-[3 (trifluoromethyl)phenyl]urea (pale green) within the ATP binding pocket of VEGFR-2.

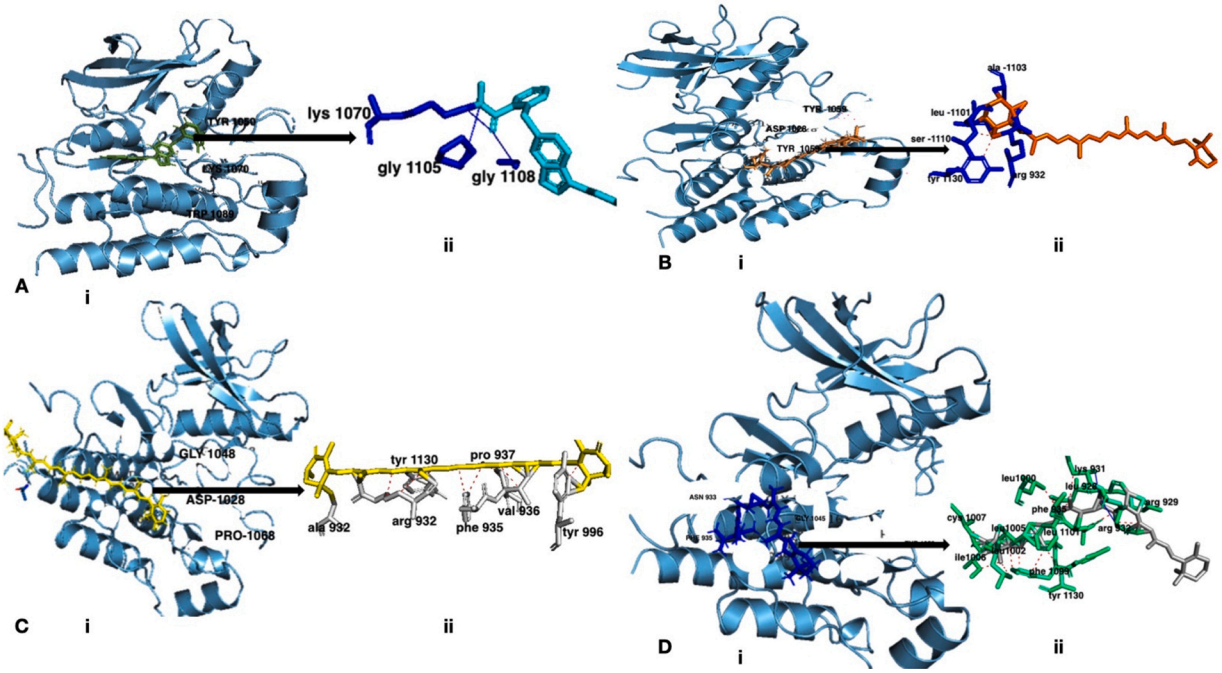

Fig. 6. A (i). VEGFR-2 kinase domain in complex with axitinib (smudge green), axitinib occupies the cleft between the N- and C-lobes of the kinase domain (the ATP binding site). Axitinib binds to the inactive state of the kinase domain with the activation loop in the "closed" conformation and the DFG motif in the "in" conformation. (ii). Interactions of axitinib (blue) within the ATP binding pocket, the blue lines represent hydrogen bonds: B (i). VEGFR-2 kinase domain in complex with 7,7′,8,8′-Tetrahydro-β,β-carotene (orange). 7,7′,8,8′-Tetrahydro-β,β-carotene occupies the cleft between the N- and C-lobes of the kinase domain (the ATP binding site) and binds to the inactive state of the kinase domain with the activation loop in the "closed" conformation and the DFG motif in the "in" conformation. (ii). Interactions of 7,7′,8,8′-Tetrahydro-β,β-carotene (orange) within the ATP binding pocket, the red lines represent hydrophobic interactions: C (i). Crystal structure of the VEGFR-2 kinase domain in complex with astaxanthin (yellow). Astaxanthin occupies the cleft between the N- and C-lobes of the kinase domain (the ATP binding site) and binds to the inactive state of the kinase domain with the activation loop in the "closed" conformation and the DFG motif in the "in" conformation. (ii). Interactions of astaxanthin (yellow) within the ATP binding pocket, the red lines represent hydrophobic interactions: D (i). Crystal structure of the VEGFR-2 kinase domain in complex with beta-Carotene-15,15′-epoxide (blue). Beta-Carotene-15,15′-epoxide occupies the cleft between the N- and C-lobes of the kinase domain (the ATP binding site) and binds to the inactive state of the kinase domain with the activation loop in the "closed" conformation and the DFG motif in the "in" conformation. (ii). Interactions of Beta-Carotene-15,15′-epoxide (gray) within the ATP binding pocket, the red lines represent hydrophobic interactions.

downregulation of the *EGFR* mRNA was greater in group 3, treated with 100 mg/kg carotenoid isolates when compared with other treatment groups (4, 5, and 6). This further confirms the fact that carotenoids at lower concentrations display greater therapeutic effects. The combination of 100 mg/kg carotenoid isolates +100 mg/kg celecoxib fails to display equivalent or marching therapeutic effects when compared with group 3 treated with 100 mg/kg carotenoid isolates. The downregulation of the expression of *VEGFR* mRNA and *EGFR* mRNA by the carotenoid isolates demonstrates the inhibition of the tyrosine kinase receptor as a likely mechanism of the downregulation.

HIF-1 displays principal roles in energy metabolism, apoptosis, angiogenesis, and control homeostatic reaction to hypoxia [35]. Elevated *HIF-1* mRNA expression is associated with poor response to treatment and prognosis [45].

The expression of *HIF-1* mRNA was significantly downregulated in all the treatment groups 3, 4, and 5 when compared with group 2. This shows the carotenoid isolates administered as a treatment in the present study possess anti-metastatic, and anti-proliferating potentials [46] since HIF-1 is known to activate these pathways.

E-cadherin (CDH1), an adhesion molecule, organizes pivotal morphogenetic processes regulating neoplastic development. A decreased level of CDH1 is a characteristic of neoplasm leading to an increase in the metastatic power of malignant cells [36]. Loss of E-cadherin function or expression is correlated with cancer progression and metastasis. Downregulation of CDH1 mRNA attenuates the firmness of cellular adhesion within a tissue, leading to cellular motility [47]. The expression of CDH1 mRNA was upregulated in the treatment groups 3, 4, and 5 when compared with group 1 and group 2. However, the upregulation of CDH1 mRNA in group 3 was not statistically significant when compared with group 2. It suffices to say that the treatments, carotenoid isolates hinder epithelial–mesenchymal transition (EMT), thereby in a way demonstrating anti-proliferative tendencies.

The *MMP-2* mRNA directs the translation of Matrix Metallopeptidase 2. They are activated through hydrolysis and cause the degradation of the basement membrane and attenuate its ability to hinder tumor cell migration. MMP-2 plays a key role in the degradation of the extracellular matrices and encouraging tumor invasion and metastasis [37]. The expression of *MMP-2* mRNA was significantly downregulated in the treatment groups except in group 3 when compared with group 2. This observation further confirms the anti-metastatic, anti-angiogenic, and antiproliferative potentials of the carotenoid isolates.

4.4. Molecular docking of the carotenoid isolates

In the present study, the phytoconstituents of the carotenoid isolates, astaxanthin, 7,7′,8,8′-tetrahydro-β,β-carotene, and beta-carotene-15,15′-epoxide docked into VEGFR-2 kinase domain, bind between the N- and C- lobes with binding energies of -8.2 kcal/mol, -10.3 kcal/mol, and -10.5 kcal/mol respectively. Astaxanthin, 7,7′,8,8′-tetrahydro-β,β-carotene, and beta-carotene-15,15′-epoxide bound to the inactive VEGFR-2 state. The mode of binding of astaxanthin, 7,7′,8,8′-tetrahydro-β,β-carotene, and beta-carotene-15,15′-epoxide are in tandem with known tyrosine kinase inhibitors, nilotinib, and ponatinib [48]. The binding of astaxanthin, 7,7′,8,8′-tetrahydro-β,β-carotene, and beta-carotene-15,15′-epoxide to the ATP binding site led to the DFG-out conformation. Astaxanthin forms hydrophobic interactions with important residues within the ATP binding site (tyr-966, val-936, phe-935, pro-937, tyr-1130, arg-932, and ala-932), 7,7′,8,8′-tetrahydro-β,β-carotene on the other hand also forms hydrophobic interactions with arg-932, tyr-1130, ser-1101, leu-1101, and ala-1103. Lastly, beta-carotene-15,15′-epoxide forms hydrophobic interactions with leu-928, arg-929, lys-921, arg-932, phe-935, leu-1000, leu 1002, leu-1005, ile-1006, cys-1007, ile-1098, phe-1099, leu-1101, and tyr-1130 and also forms hydrogen bond interaction with lys-931, and arg-932. The lowest binding energy of beta-carotene-15,15′-epoxide, -10.5 kcal/mol, when compared with astaxanthin and 7,7′,8,8′-tetrahydro-β,β-carotene is likely due to its extensive hydrophobic interactions coupled with the hydrogen bond interactions with the ATP binding domain. It is worthy of note that the binding of beta-carotene-15,15′-epoxide span through the ATP binding domain, thereby making interactions with key residues that are needed for competitive inhibition of the kinase domain. The anti-angiogenic potential demonstrated in the present study is likely due to beta-Carotene-15,15′-epoxide because of its inhibition of the VEGFR-2 kinase domain. This observation confirms the report of (Guruvayoorappan and Kuttan (2007) [49] that β-carotene inhibits angiogenesis.

The re-docking of 1-{2-fluoro-4-[(5-methyl-5H-pyrrolo[3,2-d]pyrimidin-4-yl)oxy]phenyl}-3-[3-(trifluoromethyl)phenyl]urea back into the ATP binding pocket of the VEGFR-2 (3VHE) gave RMSD value of 0.071 Å (Fig. 7) [50]. The re-docked pose overlaps with the experimental orientation, depicting that the virtual screening cum molecular docking employed in this study is accurate.

4.5. Histopathological Analysis of DMBA model of breast carcinoma

DMBA induces mammary tumor (Fig. 3) formation in an animal model [51]. Group 2 shows atypical features (pleomorphism and hyperchromasia) consistent with sarcomatoid lesions. This shows DMBA induces both sarcoma and comedo carcinoma. Comedo carcinoma of the breast is a type of ductal carcinoma in situ [52].

In group 3, the formation of invasive ductal carcinoma was also observed, this shows that in the present study DMBA induces not only comedo carcinoma but also invasive ductal carcinoma subtypes of breast cancers. The formation of extensive necrosis in group 4 is believed to be due to the treatment with 200 mg/kg body weight of the carotenoid isolates. According to Amaravadi and Thompson, (2007) [53] necrosis can be the end product of apoptosis and therapy-induced necrotic cell death has been reported to initiate an immune response to tumor cells. Conclusively, the DMBA model of breast carcinoma in the present study induced comedo and invasive ductal subtypes of breast carcinoma.

4.6. Tumour Volume in DMBA model of breast carcinoma

Determining the tumour volume is evidenced to have prognostic importance in various studies [54,55]. Treatment of DMBA-induced breast cancer (Fig. 3) with the carotenoid isolates is shown to reduce the tumour volume (Fig. 4). The reduction in the mammary tumour volume observed in this study corroborated the earlier report of Chew et al. (1999) [56] that carotenoids decreased mammary tumor volume. Solid tumor growth is reliant on angiogenesis [57], thus the decrease in mammary tumour volume is probably due to the anti-angiogenic potential of the treatment (carotenoid isolates).

5. Conclusion

The binding of carotenoid isolates of *Spondias mombin,* astaxanthin, 7,7′,8,8′-tetrahydro-β,β-carotene, and beta-carotene-15,15′-epoxide to the ATP binding site of VEGFR2 kinase domain led to the DFG-out conformation and are in tandem with known tyrosine kinase inhibitors. Treatment with the carotenoid isolates of *Spondias mombin* demonstrated anti-angiogenic and anti-proliferating potentials in the DMBA model of breast cancer.

CRediT authorship contribution statement

Damilohun Samuel Metibemu: Conceptualization, Methodology, Software, Formal analysis, Writing - original draft, Writing - review & editing. **Oluseyi Adeboye Akinloye:** Supervision, Conceptualization, Investigation, Visualization. **Adio Jamiu Akamo:** Supervision, Data curation, Investigation. **Jude Ogechukwu Okoye:** Visualization, Formal analysis, Writing - review & editing. **David Ajiboye Ojo:** Supervision, Data curation, Investigation. **Eric Morifi:** Formal analysis,

Visualization. **Idowu Olaposi Omotuyi:** Methodology, Software, Supervision.

Declaration of Competing Interest

The authors report no declarations of interest.

Acknowledgments

The authors appreciate the Mass Spectrometry Laboratory, Witwatersrand University, Johannesburg for the Liquid Chromatography-Mass Spectrometry analysis.

Appendix A. Supplementary data

Supplementary material related to this article can be found, in the online version, at doi:https://doi.org/10.1016/j.toxrep.2021.02.011.

References

[1] F. Bray, J. Ferlay, I. Soerjomataram, R.L. Siegel, L.A. Torre, A. Jemal, Global cancer statistics 2018: GLOBOCAN estimates of incidence and mortality worldwide for 36 cancers in 185 countries, CA: CA Cancer J. Clin. 68 (6) (2018) 394–424.
[2] L. Lian, X.L. Li, M.D. Xu, X.M. Li, M.Y. Wu, Y. Zhang, M. Jiang, VEGFR2 promotes tumorigenesis and metastasis in a pro-angiogenic-independent way in gastric cancer, BMC Cancer 19 (1) (2019) 183.
[3] M. Simons, E. Gordon, L. Claesson-Welsh, Mechanisms and regulation of endothelial VEGF receptor signalling, Nat. Rev. Mol. 17 (10) (2016) 611.
[4] H.L. Goel, A.M. Mercurio, VEGF targets the tumour cell, Nat. Rev. Cancer 13 (12) (2013) 871–882, https://doi.org/10.1038/nrc3627.
[5] D.S. Metibemu, O.A. Akinloye, A.J. Akamo, D.A. Ojo, O.T. Okeowo, I.O. Omotuyi, Exploring receptor tyrosine kinases-inhibitors in cancer treatments, Egypt. J. Med. Hum. Genet. 20 (1) (2019) 1–16.
[6] E. Kilic, U. Kilic, Y. Wang, C.L. Bassetti, H.H. Marti, D.M. Hermann, The phosphatidylinositol-3 kinase/Akt pathway mediates VEGF's neuroprotective activity and induces blood brain barrier permeability after focal cerebral ischemia, FASEB 20 (8) (2006) 1185–1187, https://doi.org/10.1096/fj.05-4829fje.
[7] G. Niu, X. Chen, Vascular endothelial growth factor as an anti-angiogenic target for cancer therapy, Curr. Drug Targets 11 (8) (2010) 1000–1017, https://doi.org/10.2174/138945010791591395.
[8] K. Lu, M. Bhat, S. Basu, Plants and their active compounds: natural molecules to target angiogenesis, Angiogenesis 19 (3) (2021) 287–295, https://doi.org/10.1007/s10456-016-9512-y.
[9] A.G. Atanasov, B. Waltenberger, E.M. Pferschy-Wenzig, T. Linder, C. Wawrosch, P. Uhrin, V. Temml, et al., Discovery and resupply of pharmacologically active plant-derived natural products: a review, Biotechnol. Adv. 33 (8) (2015) 1582–1614, https://doi.org/10.1016/j.biotechadv.2015.08.001.
[10] S. Chirumbolo, G. Bjørklund, R. Lysiuk, A. Vella, L. Lenchyk, T. Upyr, Targeting cancer with phytochemicals via their fine tuning of the cell survival signaling pathways, Int. J. Mol. Sci. 19 (11) (2018) 3568.
[11] A. Zwartsen, S. Chottanapund, P. Kittakoop, P. Navasumrit, M. Ruchirawat, M.B. M. Van Duursen, M. Van den Berg, Evaluation of anti-tumour properties of two depsidones–Unguinol and Aspergillusidone D–in triple-negative MDA-MB-231 breast tumour cells, Toxicol. Rep. 6 (2020) 1216–1222.
[12] I.J. Enyedy, W.J. Egan, Can we use docking and scoring for hit-to-lead optimization? J Comput. Aided Mol. Des. 22 (2008) 161–168.
[13] U. Rester, From virtuality to reality – virtual screening in lead discovery and lead optimization: a medicinal chemistry perspective, Curr. Opin. Drug Discov. Devel. 11 (4) (2008) 559–568.
[14] O.E. Fadeyi, G.A. Olatunji, V.A. Ogundele, Isolation and characterization of the chemical constituents of *Anacardium occidentale* cracked bark, Nat. Prod. Chem. Res. 3 (2015) 5.
[15] M.P. Venuprasad, H. Kumar Kandikattu, S. Razack, F. Khanum, Phytochemical analysis of Ocimum gratissimum by LC-ESI–MS/MS and its antioxidant and anxiolytic effects, S. Afr. J. Bot. 92 (2014) 151–158.
[16] A.F. Akinmoladun, M.F. Khan, J.S. Sarkar, E.O. Farombi, R. Maurya, Distinct radical scavenging and antiproliferative properties of *Spondias mombin* and antioxidant activity-guided isolation of quercetin-3-O-β-D- glucopyranoside and undec-1-ene, Afr. J. Pharm. Pharmacol. 9 (17) (2015) 506–513.
[17] H.Y.K. Kim, S.-Y. Mok, S.H. Kwon, D.G. Lee, E.J. Cho, S. Lee, Phytochemical constituents of bitter melon (*Momordica charantia*), News Physiol. Sci. 19 (4) (2012) 286–289.
[18] M.C. Ojinnaka, S.C. Ubbor, H.O. Okudu, U. Uga, Volatile compound analysis of the leaves and seeds of Piper guineense using gas chromatography-mass spectrometry (GC-MS), Afr. J. Food Sci. Technol. 10 (11) (2016) 327–332.
[19] C. Imo, F.O. Uhegbu, Phytochemical analysis of Gongronema latifolium benth leaf using gas chromatographic flame ionization detector, Int. J. Chem. Biomol. Sci. 2 (2015) 60–68.
[20] Y. Oguro, N. Miyamoto, K. Okada, T. Takagi, H. Iwata, Y. Awazu, et al., Design, synthesis, and evaluation of 5-methyl-4-phenoxy-5H-pyrrolo[3,2-d] pyrimidine derivatives: novel VEGFR2 kinase inhibitors binding to inactive kinase conformation, Bioorg. Med. Chem. 18 (20) (2010) 7260–7273.
[21] G.A. Rodriguez, Extraction, isolation, and purification of carotenoids, Curr. Protcl. Food Analyt. Chem. 00 (1) (2001) F2.1.1–F2.1.8.
[22] D.S. Metibemu, O.A. Akinloye, A.J. Akamo, J.O. Okoye, D.A. Ojo, E. Morifi, I. O. Omotuyi, Carotenoid isolates of *Spondias mombin* demonstrate anticancer effects in DMBA-induced breast cancer in Wistar rats through X-linked inhibitor of apoptosis protein (XIAP) antagonism and anti-inflammation, J. Food Biochem. (2020) e13523.
[23] F. Faul, E. Erdfelder, A. Buchner, A.G. Lang, Statistical power analyses using G*Power 3.1: tests for correlation and regression analyses, Behav. Res. Methods 41 (2009) 1149–1160.
[24] C. Costa, R. Soares, J.S. Reis-Filho, D. Leitão, I. Amendoeira, F.C. Schmitt, Cyclo-oxygenase 2 expression is associated with angiogenesis and lymph node metastasis in human breast cancer, J. Clin. Pathol. 55 (6) (2002) 429–434, https://doi.org/10.1136/jcp.55.6.429.
[25] S.M. Anbazahan, L.S. Mari, G. Yogeshwari, C. Jagruthi, R. Thirumurugan, J. Arockiaraj, et al., Immune response and disease resistance of carotenoids supplementation diet in Cyprinus carpio against Aeromonas hydrophila, Fish Shellfish Immun. 40 (1) (2021) 9–13.
[26] A.C. Barros, E.N. Muranaka, L.J. Mori, C.H. Pelizon, K. Iriya, G. Giocondo, J. A. Pinotti, Induction of experimental mammary carcinogenesis in rats with 7,12-dimethylbenz(a)anthracene, Rev. Hosp. Clin. 59 (5) (2004) 257–261.
[27] R.S. Geran, N.H. Greenberg, M.M. Macdonald, A.M. Schumacher, B.J. Abbott, Protocols for screening chemical agents and natural products against animal tumors and other biological systems, Cancer Chemother. Rep. 13 (1972) 1–87.
[28] X. Zhao, X.X. Deng, K.Y. Park, L.H. Qiu, L. Pang, Purple bamboo salt has anticancer activity in TCA8113 cells in vitro and preventive effects on buccal mucosa cancer in mice in vivo, Exp. Ther. Med. 5 (2013) 549–554.
[29] F. Allen, R. Greiner, D. Wishart, Competitive fragmentation modeling of ESI-MS/MS spectra for putative metabolite identification, Metabolomics 11 (1) (2015) 98–110.
[30] M. Magrane, UniProt Knowledgebase: A Hub of Integrated Protein Data. Database, 2011.
[31] D.S. Wishart, Y.D. Feunang, A. Marcu, A.C. Guo, K. Liang, R. Vázquez-Fresno, et al., HMDB 4.0: the human metabolome database for 2018, Nucleic Acids Res. 46 (D1) (2017) D608–D617.
[32] P. Carmeliet, VEGF as a key mediator of angiogenesis in cancer, Oncology 69 (3) (2005) 4–10.
[33] L. Rydén, B. Linderholm, N.H. Nielsen, S. Emdin, P.-E. Jönsson, G. Landberg, Tumor specific VEGF-A and VEGFR2/KDR protein are co-expressed in breast cancer, Breast Cancer Res. Treat. 82 (3) (2003) 147–154.
[34] J. Baselga, Why the epidermal growth factor receptor? The rationale for cancer therapy, Oncologist 7 (suppl 4) (2002) 2–8.
[35] Y.B. Xie, J.P. Li, K. Shen, F. Meng, L. Wang, G.X. Han, et al., Effect of HIF-1α on angiogenesis-related factors in K562 cells, Zhongguo Shi Yan Xue Ye Xue Za Zhi 27 (5) (2019) 1476–1481.
[36] M.E. Lindberg, G.R. Stodden, M.L. King, J.A. MacLean, J.L. Mann, F.J. DeMayo, et al., Loss of CDH1 and Pten accelerates cellular invasiveness and angiogenesis in the mouse uterus, Biol. Reprod. 89 (1) (2013) 8.
[37] Y. Nishida, H. Miyamori, E.W. Thompson, T. Takino, Y. Endo, H. Sato, Activation of matrix metalloproteinase-2 (MMP-2) by membrane type 1 matrix metalloproteinase through an artificial receptor for proMMP-2 generates active MMP-2, Cancer Res. 68 (21) (2008) 9096–9104.
[38] T. Tanaka, Effect of diet on human carcinogenesis, Crit. Rev. Oncol. Hematol. 25 (1997) 73–95.
[39] K. Linnewiel-Hermoni, M. Khanin, M. Danilenko, G. Zango, Y. Amosi, J. Levy, Y. Sharoni, The anti-cancer effects of carotenoids and other phytonutrients resides in their combined activity, Arch. Biochem. Biophys. 572 (2015) 28–35.
[40] G. Sliwoski, S. Kothiwale, J. Meiler, E.W. Lowe Jr., Computational methods in drug discovery, Pharmacol. Rev. 66 (1) (2013) 334–395.
[41] I. Blaženović, T. Kind, J. Ji, O. Fiehn, Software tools and approaches for compound identification of LC-MS/MS data in metabolomics, Metabolites 8 (2) (2018) 31.
[42] C.R. Pradeep, E.S. Sunila, G. Kuttan, Expression of vascular endothelial growth factor (VEGF) and VEGF receptors in tumor angiogenesis and malignancies, Integr. Cancer Ther. 4 (4) (2005) 315–321.
[43] S. Kuhnen, P.M.M. Lemos, L.H. Campestrini, J.B. Ogliari, P.F. Dias, M. Maraschin, Antiangiogenic properties of carotenoids: a potential role of maize as functional food, J. Funct. Foods 1 (3) (2009) 284–290.
[44] N. Normanno, A. De Luca, C. Bianco, L. Strizzi, M. Mancino, M.R. Maiello, et al., Epidermal growth factor receptor (EGFR) signaling in cancer, Gene 366 (1) (2006) 2–16.
[45] G.N. Masoud, W. Li, HIF-1α pathway: role, regulation and intervention for cancer therapy, Acta Pharm. Sin. B 5 (5) (2015) 378–389.
[46] X. Gong, J.R. Smith, H.M. Swanson, L.P. Rubin, Carotenoid lutein selectively inhibits breast cancer cell growth and potentiates the effect of chemotherapeutic agents through ROS-Mediated mechanisms, Molecules 23 (4) (2018) 905.
[47] A. Techasen, W. Loilome, N. Namwat, N. Khuntikeo, A. Puapairoj, P. Jearanaikoon, et al., Loss of E-cadherin promotes migration and invasion of cholangiocarcinoma cells and serves as a potential marker of metastasis, Tumour Biol. 35 (9) (2014) 8645–8652.
[48] E.P. Reddy, A.K. Aggarwal, The ins and outs of bcr-abl inhibition, Genes Cancer 3 (5–6) (2012) 447–454.
[49] C. Guruvayoorappan, G. Kuttan, β-carotene inhibits tumor-specific angiogenesis by altering the cytokine profile and inhibits the nuclear translocation of transcription factors in B16F-10 melanoma cells, Integr. Cancer Ther. 6 (3) (2007) 258–270.

[50] G.M. Morris, D.S. Goodsell, R.S. Halliday, R. Huey, W.E. Hart, R.R. Belew, A. J. Olson, Automated docking using a Lamarckian genetic algorithm and an empirical binding free energy function, J. Comput. Chem. 19 (1998) 1639–1662.
[51] Z. Liu, T. Kundu-Roy, I. Matsuura, G. Wang, Y. Lin, Y.R. Lou, et al., Carcinogen 7,12-dimethylbenz[a]anthracene-induced mammary tumorigenesis is accelerated in Smad3 heterozygous mice compared to Smad3 wild type mice, Oncotarget 7 (40) (2016) 64878–64885.
[52] M.P. Shekhar, L. Tait, R.J. Pauley, G.S. Wu, S.J. Santner, P. Nangia-Makker, Comedo-ductal carcinoma in situ: a paradoxical role for programmed cell death, Cancer Biol. Ther. 7 (11) (2008) 1774–1782.
[53] R.K. Amaravadi, C.B. Thompson, The roles of therapy-induced autophagy and necrosis in cancer treatment, Clin. Cancer Res. 13 (24) (2007) 7271–7279.
[54] M. Feng, W. Wang, Z. Fan, B. Fu, J. Li, S. Zhang, J. Lang, Tumor volume is an independent prognostic indicator of local control in nasopharyngeal carcinoma patients treated with intensity-modulated radiotherapy, Radiat. Oncol. 8 (1) (2013) 208.
[55] Z. Wu, R.F. Zeng, Y. Su, M.F. Gu, S.M. Huang, Prognostic significance of tumor volume in patients with nasopharyngeal carcinoma undergoing intensity-modulated radiation therapy, Head Neck 35 (5) (2013) 689–694.
[56] B.P. Chew, J.S. Park, M.W. Wong, T.S. Wong, A comparison of the anticancer activities of dietary beta-carotene, canthaxanthin and astaxanthin in mice in vivo, Anticancer Res. 19 (3A) (1999) 1849–1853.
[57] W.W. Li, V.W. Li, M. Hutnik, A.S. Chiou, Tumor angiogenesis as a target for dietary cancer prevention, J. Oncol. (2012) 1–23.